1   Pseudorabies Virus Infection Accelerates Degradation of the Kinesin-3 Motor KIF1A

2

3   Running Title: Pseudorabies Virus Accelerates KIF1A Degradation

4

5   Hao Huang[a], Orkide O. Koyuncu[a], and Lynn W. Enquist[a#].

6

7   [a]Department of Molecular Biology, Princeton University, Princeton, New Jersey, USA

8   [#]Corresponding author: Lynn W. Enquist, lenquist@princeton.edu

9

10   Word Count: Abstract (231),

11   Main Text (5744)

12   Keywords: alphaherpesvirus, pseudorabies virus, kinesin, KIF1A, proteasomal degradation,

13   axonal sorting.

14

15

16

Abstract

Alphaherpesviruses, including pseudorabies virus (PRV), are neuroinvasive pathogens that establish life-long latency in peripheral ganglia following the initial infection at mucosal surfaces. The establishment of latent infection and the subsequent reactivations during which newly-assembled virions are sorted into and transported anterogradely inside axons to the initial mucosal site of infection, rely on axonal bidirectional transport mediated by microtubule-based motors. Previous studies using cultured peripheral nervous system (PNS) neurons have demonstrated that KIF1A, a kinesin-3 motor, mediates the efficient axonal sorting and transport of newly-assembled PRV virions. In this study, we report that KIF1A, unlike other axonal kinesins, is an intrinsically unstable protein prone to proteasomal degradation. Interestingly, PRV infection of neuronal cells leads not only to a non-specific depletion of KIF1A mRNA, but also to an accelerated proteasomal degradation of KIF1A proteins, leading to a near depletion of KIF1A protein late in infection. Using a series of PRV mutants deficient in axonal sorting and anterograde spread, we identified the PRV US9/gE/gI protein complex as a viral factor facilitating the proteasomal degradation of KIF1A proteins. Moreover, by using compartmented neuronal cultures that fluidically and physically separate axons from cell bodies, we found that the proteasomal degradation of KIF1A occurs in axons during infection. We propose that PRV anterograde sorting complex, gE/gI/US9, recruits KIF1A to viral transport vesicles for axonal sorting and transport, and eventually accelerates the proteasomal degradation of KIF1A in axons.

36 **Importance**

37 Pseudorabies virus (PRV) is an alphaherpesvirus related to human pathogens herpes simplex

38 virus -1, -2 and varicella zoster virus. Alphaherpesviruses are neuroinvasive pathogens that

39 establish life-long latent infections in the host peripheral nervous system (PNS). Following

40 reactivation from latency, infection spreads from the PNS back via axons to the peripheral

41 mucosal tissues, a process mediated by kinesin motors. Here, we unveil and characterize the

42 underlying mechanisms for a PRV-induced, accelerated degradation of KIF1A, a kinesin-3

43 motor promoting the sorting and transport of PRV virions in axons. We show that PRV infection

44 disrupts the synthesis of KIF1A, and simultaneously promotes the degradation of intrinsically

45 unstable KIF1A proteins by proteasomes in axons. Our work implies that the timing of motor

46 reduction after reactivation would be critical because progeny particles would have a limited

47 time window for sorting into and transport in axons for further host-to-host spread.

3

48 **Introduction**

49

50   Alphaherpesviruses, including human pathogens herpes simplex virus-1 and -2, varicella-zoster

51   virus, and the veterinary pathogen pseudorabies virus (PRV), are neuroinvasive pathogens that

52   establish and maintain life-long latency in the sensory and automatic ganglia of the peripheral

53   nervous system (PNS) of their mammalian hosts following initial infection at mucosal surfaces (1-

54   3). Latently infected neurons in peripheral ganglia undergo occasional reactivation, during which

55   viral genomes are actively replicated and new viral particles assembled. Spread of infection to new

56   hosts requires that these progeny virions be transported to the initial site of epithelial infection,

57   where replication and subsequent host-to-host transmission occur. On rare occasions, infection

58   spreads from the PNS to the central nervous system, often with serious consequences such as

59   herpes simplex encephalitis (HSE).

60

61   Axonal bidirectional transport mechanisms are crucial for the virions and virus proteins to move

62   efficiently through the PNS axons, which are often centimeters to meters long (4). In uninfected

63   neurons, microtubule-based motors, including minus-ended directed cytoplasmic dynein and plus-

64   ended directed kinesin superfamily motors, mediate fast axonal transport of RNAs, proteins,

65   organelles, and vesicles between cell bodies and axonal termini for the maintenance and proper

66   functioning of axons (5, 6). Neuroinvasive viruses such as the alphaherpesviruses and rabies virus

67   have evolved to adopt existing axonal transport machinery for efficient neuroinvasion and

68   subsequent spread to new hosts. A notable example is rabies virus (RABV), whose phosphoprotein

69   (P) binds to LC8 dynein light chain, and was shown to hijack the P75NTR-dependent transport to

70   facilitate fast retrograde axonal transport in sensory DRG neurons (7).

71

72   Initially after infection of peripheral tissues, alphaherpesvirus virions bind to PNS axon terminals,

73   and viral capsids are released into axons where they recruit cytoplasmic dynein, via inner tegument

74   proteins UL36 and UL37 (8, 9). This complex then moves in the MT minus-end direction towards

75   the cell body and deposits the viral DNA inside the nucleus. After reactivation of a latent PNS

76   infection, kinesin-superfamily motors are recruited both for viral egress at cell bodies, as well as

77   for sorting into axons and subsequent transport of viral structural proteins and newly-assembled

78   virions (10-14). Previous studies in sympathetic PNS neurons revealed that a subpopulation of

79   fully-enveloped PRV virions in transport vesicles recruit KIF1A, a kinesin-3 motor, through the

80   interactions with a gE/gI/US9 tripartite membrane protein complex in lipid rafts at late Golgi

81   network compartments (e.g., late endosomes or the trans-Golgi network (TGN)) (14, 15). After

82   this interaction, fully enveloped virions in transport vesicles are sorted into axons followed by

83   unidirectional anterograde transport before egressing along the axonal shaft (16). In PRV infected

84   neurons, ectopic expression of dominant-negative KIF1A proteins significantly reduced the

85   number of PRV particles transported in the anterograde direction, demonstrating the critical role

86   of KIF1A in sorting virus particles into axons and also in subsequent transport (14). In this report,

87   we focus on a curious observation made by Kramer et al, who noted that the amount of KIF1A in

88   infected cultured neuronal cells decreased significantly late after PRV infection (14).

89

90   In uninfected neurons, the kinesin motor KIF1A mediates fast axonal transport of membranous

91   vesicles including synaptic vesicle precursors and dense core vesicles, and is critical in dendrite

92   morphogenesis and synaptogenesis (17-19). Neurons lacking KIF1A showed impaired transport

93   in synaptic vesicle precursors, marked neuronal degeneration, and death in both cultured neurons

5

94   and *in vivo* (20). Despite its functional importance, several lines of evidence suggest that KIF1A

95   motors are degraded upon the completion of their axonal transportation runs, and are not recycled

96   for further use. Studies with a ligature applied to the mouse sciatic nerve revealed increased

97   antibody staining of KIF1A in the proximal (close to the cell body), but not distal (close to the

98   axonal terminal), region of ligature, suggesting that once KIF1A motors entered axons, they did

99   not return to the cell bodies (e.g. with dyneins) (21). UNC-104, the KIF1A homolog in *C. elegans*,

100   was shown to be degraded by ubiquitin-related pathways at synapses of mechanosensory neurons

101   (22). More importantly, the stability of UNC-104 protein strongly correlates with the motor's

102   specific binding to cargo, implying a potential mechanistic link between motor degradation and

103   cargo release (22).

104

105   In this study, we investigated KIF1A protein dynamics during PRV infection both in neuronal cell

106   lines and in primary neurons. Here, we report that KIF1A (kinesin-3), unlike kinesin-1 and kinesin-

107   2 motors, is intrinsically prone to proteasomal degradation in uninfected neuronal cells. We further

108   showed that PRV infection blocks new synthesis of this motor, and that viral anterograde-sorting

109   complex US9/gE/gI specifically targets KIF1A for proteasomal degradation, resulting in a near

110   depletion of the protein in 24 hours following infection. Using compartmented neuronal cultures

111   that fluidically and physically separate axons from cell bodies, we found that the proteasomal

112   degradation of KIF1A proteins occurs in axons. Moreover, using a series of PRV mutants deficient

113   in anterograde spread, and using adenovirus vectors to express the viral proteins in neuronal cells,

114   we discovered that the PRV US9/gE/gI protein complex targets specifically KIF1A motors for

115   proteasomal degradation. Altogether, these results suggest that progeny PRV particles recruit

116   KIF1A motors for efficient axonal sorting and anterograde transport that leads to the degradation

117   of the motor protein in axons. Since new synthesis of KIF1A is also blocked by PRV infection,

118   these results suggest progeny particles have a limited time window for sorting into and transport

119   in axons for further host-to-host spread.

120

121   **Results**

122

123   **In uninfected, differentiated PC12 cells, the steady state concentration of KIF1A protein is**

124   **achieved through rapid protein synthesis and proteasomal degradation.**

125

126   We tested the hypothesis that in differentiated PC12 cells axonal kinesins undergo rapid

127   degradation while protein synthesis continues. To determine the role of the proteasome in this

128   process, we treated uninfected differentiated PC12 cells with the proteasomal inhibitor MG132 for

129   2, 4, 6, and 8 hours, and monitored the protein concentration of three different kinesin motors:

130   KIF5 (kinesin-1, and the conventional kinesin), KIF3A (kinesin-2), and KIF1A (kinesin-3).

131   MG132 treatment led to more than a 2-fold increase in KIF1A concentration within 6 hours post

132   treatment, indicating that KIF1A protein rapidly accumulated upon proteasome inhibition (Figure

133   1A and B). However, this surge in KIF1A concentration was ablated when PC12 cells were

134   simultaneously treated with MG132 and cycloheximide, a protein synthesis inhibitor, and KIF1A

135   concentration remained at the similar levels as in untreated cells. These experiments demonstrated

136   that KIF1A proteins are degraded by the proteasomes with new proteins efficiently made to

137   maintain protein steady state levels. Consistent with this idea, in cells treated with CHX alone,

138   KIF1A concentration dropped by over 50% within 4 hours of treatment (Figure 1A and B).

139

140   In contrast to KIF1A, neither KIF5 nor KIF3A protein concentration increased significantly during

141   MG132 treatment (Figure 1A, C and D). With both MG132 and CHX treatments, KIF5 and KIF3A

142   concentrations appeared unchanged in the 8 h treatment period (Figure 1A, C and D), suggesting

143   that while both proteins are degraded by proteasomes, their rate of degradation is much slower

144   than that of KIF1A. As a result, the half-lives of both KIF5 and KIF3A proteins were much longer

145   (> 8 hours) than the half-life of KIF1A in CHX-treated PC12 cells.

146

147   **PRV infection induces specific reduction of KIF1A protein late in infection**

148

149   The inherent instability of KIF1A in uninfected cells prompted us to explore an observation

150   previously made in our laboratory: the concentration of KIF1A protein, the major kinesin

151   facilitating axonal sorting and transport of PRV virions, decreased late in PRV infection of

152   sympathetic neuronal cells. This observation might explain the significant numbers of immobile

153   PRV particles in axons late in infection (23). Accordingly, we infected differentiated PC12 cells

154   with PRV Becker at an MOI of 20 for 3, 8, 12, 16, 20, and 24 hours, and monitored KIF1A protein

155   levels by quantitative western blot methods. Similar to the previous report, we found that the

156   KIF1A protein concentration dropped by ~90% at 24 hpi (Figure 2A and B, Figure S1). To

157   determine if PRV infection affects the steady state concentrations of other kinesin motors, we

158   monitored the protein levels of KIF5 and KIF3A, two kinesins well-characterized in mediating

159   axonal transport. Neither KIF5 nor KIF3A protein levels were affected by PRV infection (Figure

160   2).

161

162   **PRV infection reduces both KIF1A and KIF5B transcripts.**

8

163

164   Alphaherpesviruses promote the instability of many host cell transcripts early in infection, leading

165   to reduced protein synthesis (24-27). We hypothesized that the loss of KIF1A proteins in PRV-

166   infected PC12 cells resulted from such mRNA degradation. We therefore measured the amounts

167   of KIF1A transcripts in PRV infected cells by qRT-PCR. Differentiated PC12 cells were infected

168   with PRV Becker and the attenuated vaccine strain PRV Bartha at an MOI of 20 for 3, 8, 12, 16,

169   20, 24 hours. Infected cells were collected for RNA extraction and qRT-PCR analysis of KIF1A,

170   KIF5B, and GAPDH mRNA level (Figure 3). In PRV Becker-infected cells, we detected a

171   significant and uniform reduction of KIF1A, KIF5B, and GAPDH transcripts as early as 8 hpi, and

172   their respective concentrations dropped by more than 80% at 16 hpi (Figure 3A).

173

174   Compared to PRV Becker infection, PRV Bartha infection decreased KIF1A transcripts at a slower

175   rate, starting at 12 hpi, with more than 80% loss at 20 hpi (Figure 3B). Reduction of GAPDH and

176   KIF5B transcripts occurred with comparable rates and magnitude to the KIF1A transcripts. These

177   experiments showed that KIF1A transcripts were reduced in PRV-infected PC12 cells, but with

178   different kinetics after infection by different PRV strains. Such transcriptional regulation may be

179   one reason why KIF1A protein levels drop significantly during PRV infection. However, this

180   effect was not specific for KIF1A, because KIF5B transcripts were also reduced after infection.

181   Therefore, the specific loss of KIF1A and not KIF5B proteins in infected neurons is not due to

182   reduction of transcript levels.

183

184   **KIF1A is degraded by the proteasome during PRV infection in differentiated PC12 cells and**

185   **in primary SCG neurons.**

186   We found that KIF1A (but not other kinesins) is rapidly degraded by the proteasome in uninfected

187   PC12 cells. We also knew from previous studies that complexes of PRV US9 and KIF1A contain

188   the E3-ubiquitin ligases NEDD4 and EP0, suggesting that KIF1A may be degraded via the

189   ubiquitin-proteasome pathway after PRV infection (14). To examine this possibility, we infected

190   differentiated PC12 cells with PRV Becker at an MOI of 20, followed by treatment with the

191   proteasomal inhibitor MG132 at 12 hpi. In mock-infected cells, KIF1A proteins accumulated

192   rapidly, doubling the concentration in 8 hours, after MG132 treatment (Figure 4A and C). However,

193   in PRV Becker infected cells, MG132 treatment led to an effective stabilization of KIF1A protein

194   levels where the protein concentration remained mostly unchanged during the treatment period

195   (Figure 4B and C). This finding suggests that, in the late phase of infection, new KIF1A synthesis

196   is blocked but proteasomal degradation continues, leading to the accelerated loss of KIF1A during

197   PRV infection.

198

199   These studies were done in differentiated PC12 cells that have similar attributes to sympathetic

200   neurons. We performed similar experiments in primary rat superior cervical ganglionic neurons

201   (SCG) cultured in compartmented chambers where we could examine kinesin motor concentration

202   in isolated axons. We cultured primary sympathetic rat SCG neurons in trichambers, in which

203   axons (in the neurite compartment, N) were fluidically and physically separated from cell bodies

204   (in the soma compartment, S) (Figure 5A). SCG cell bodies in the S compartment were infected

205   with PRV Becker for 24 hours and extracts from the S and N compartments were collected for

206   western blot analysis. The concentration of KIF1A protein decreased dramatically both in cell

207   bodies and axons after PRV infection (Figure 5B).

208

10

209 We further determined if the loss of KIF1A protein is mediated by proteasomes in isolated SCG

210 axons during infection. SCG neurons cultured in trichambers were infected with PRV Becker in

211 the S compartment, followed by MG132 treatment in the N compartment at 8 hpi. KIF1A protein

212 levels were reduced significantly in both S and N compartments after PRV Becker infection

213 (Figure 5C). Moreover, axonal KIF1A levels were partially restored by MG132 treatment in the

214 N-compartment (Figure 5C). We concluded that PRV infection accelerates the degradation of

215 KIF1A proteins by proteasomes in axons.

216

217 **Expression of both PRV early and late genes are involved in accelerated KIF1A degradation**

218 **during infection.**

219

220 We next searched for viral proteins that might accelerate KIF1A protein degradation. First, we

221 determined if early events such as virion entry and tegument protein delivery would be enough to

222 promote KIF1A degradation. We infected PC12 cells either with UV treated PRV Becker virions

223 (UVPRV) or with a PRV mutant that lacks IE180 (PRV HKO146), the single master immediate

224 early transcriptional activator of viral genes required for RNA transcription and DNA replication

225 (28, 29). Both UVPRV and PRV HKO146 (grown in IE180-complementing cells) enter the cells,

226 release outer tegument proteins (including vhs, the virion host shutoff protein), and deposit viral

227 DNA in the nucleus, but neither can initiate *de novo* viral protein synthesis. We found that after

228 either infection, KIF1A was not degraded (Figure 6A). We concluded that PRV entry into PC12

229 cells is not sufficient to accelerate KIF1A protein degradation.

230

11

231   We next determined if PRV immediate-early and early, or late genes were involved in KIF1A

232   protein degradation. We pretreated differentiated PC12 cells with the herpesvirus DNA replication

233   inhibitor AraT for 15 minutes, and infected them with PRV Becker for 8, 12, 16, 20, 24 hours.

234   AraT inhibition should have minimal effects on early viral gene expression, but should severely

235   diminish late gene expression. As expected, we detected comparable amounts of the early protein,

236   EP0, in both AraT treated and untreated cells during infection, whereas the accumulation of the

237   late protein VP5 (also major capsid protein, MCP) was severely affected by the AraT treatment

238   (Figure 6B). AraT treatment led to a minor, though statistically significant, stabilization of KIF1A

239   protein in the later stage of infection (Figure 6B-C). This experiment demonstrated that while PRV

240   IE and/or E gene products could promote a reduction in KIF1A protein levels (e.g. potentially

241   through the reduction of KIF1A transcripts), viral proteins accumulating in the late phase of

242   infection are also required for efficient degradation of KIF1A.

243

244   **PRV anterograde-sorting complex US9/gE/gI promotes the accelerated degradation of**

245   **KIF1A proteins.**

246

247   PRV particles in transport vesicles use KIF1A for sorting into axons and subsequent transport. The

248   recruitment of KIF1A to transport vesicles containing enveloped PRV particles at the TGN

249   requires viral membrane protein US9. This interaction is stabilized by the heterodimer of gE/gI.

250   We had noted previously that two ubiquitin ligases, NEDD4 and viral EP0, co-purified with US9

251   and KIF1A (14). Since KIF1A instability results from proteasomal degradation, we hypothesized

252   that the tripartite complex US9/gE/gI might be involved in accelerating KIF1A degradation. We

253   infected differentiated PC12 cells with PRV Becker and two PRV mutants that were deleted for

254   US9, gE, and gI genes, and are deficient in axonal sorting and anterograde spread: PRV Bartha

255   and PRV BaBe (PRV Becker with the Us region of Bartha). Infection with either mutant lacking

256   US9, gE, and gI partially restored KIF1A proteins during PRV infection (Figure 7A and B). As

257   both of these mutant viruses degrade host transcripts presumably through early proteins, KIF1A

258   levels show a comparable decrease between 8-12 hpi to Becker infection. However, we did not

259   detect the rapid decrease in KIF1A protein levels after 12 h in Bartha and BaBe infections,

260   suggesting that the tripartite complex help accelerate the degradation of KIF1A by proteasomes

261   (Figure 1A and B). We further infected PC12 cells with two PRV US9 mutants deficient in

262   anterograde spread, PRV 161 (US9-null), and PRV 172 (Y49-50A US9, functionally null). In

263   PRV172 infections, all US9, gE, and gI proteins were present, but the dityrosine mutation within

264   the acidic cluster of US9 gene disrupted the formation of the tripartite complex, and made the virus

265   particles incapable of recruiting KIF1A and anterograde spread (14, 30, 31). Both PRV 161 and

266   PRV 172 infections restored KIF1A proteins in magnitudes comparable to infections with PRV

267   Bartha and Babe (Figure 7A and B). These results suggested that the formation of the tripartite

268   complex is necessary for the accelerated loss of KIF1A proteins.

269

270   We further determined if the US9/gE/gI complex could target KIF1A for degradation independent

271   of PRV infection. We transduced differentiated PC12 cells with adenovirus vectors expressing the

272   US9, gE, and gI protein, either individually or in combination, for 1, 2, 3, 4, 5 days. Neither the

273   control Ad-GFP nor Ad-GFP-US9 transduction resulted in KIF1A protein instability, but when

274   PC12 cells were transduced with equal units of the three adenovirus vectors expressing US9, gE,

275   and gI, the KIF1A protein was completely degraded by 5 days post transduction (Figure 7C and

13

276   Figure S2). We concluded that a functional anterograde sorting complex could augment the

277   proteasomal degradation of KIF1A protein independent of infection by PRV.

278   Altogether these results suggest that PRV infection leads to the depletion of KIF1A proteins in

279   infected neurons both by blocking new protein synthesis and also specifically targeting the motor

280   for anterograde spread of progeny late in infection, which eventually accelerates proteasomal

281   degradation of KIF1A.

282

283   **Discussion**

284

285   A major distinction of alphaherpesviruses from most of other neuroinvasive viruses is their ability

286   to travel in both anterograde and retrograde directions in axons and in neuronal circuits (4). The

287   anterograde transport of newly assembled herpesvirus virions is crucial for the viral life cycle

288   because it ensures that virus particles are sorted into axons to facilitate inter-host transmission.

289   KIF1A mediates the sorting and transport of PRV egressing virions in axons, with the dynamics

290   of transport involving long segment runs with high velocity (Vmax ~2.4μm/s) (16). The

291   anterograde transport of PRV virions was greatly hindered in the neurons expressing the dominant-

292   negative form of KIF1A protein (14). In this study, we demonstrated that KIF1A is intrinsically

293   prone to degradation by the proteasomes, and that PRV infection accelerates such degradation and

294   results in near depletion late in infection. The steady state concentration of KIF1A protein in

295   uninfected neuronal cells is achieved through rapid protein synthesis and proteasomal degradation.

296   Upon PRV infection, KIF1A mRNA was degraded in a nonspecific manner, reducing KIF1A

297   protein synthesis while the existing proteins were gradually degraded by the proteasome. In

298   addition, adenovirus vectors expressing proteins constituting the PRV anterograde sorting

14

299   complex US9/gE/gI induced a decline in KIF1A protein level independent of PRV infection,

300   suggesting the US9/gE/gI tripartite complex accelerates the proteasomal degradation of KIF1A

301   and contributes, alongside PRV host shutoff, to the decline in KIF1A protein during PRV infection.

302   Importantly, using compartmented primary neuron cultures we showed that proteasomal

303   degradation of KIF1A is accelerated in axons after PRV infection.

304

305   **The intrinsic instability of the KIF1A protein.**

306

307   The kinesin motor KIF1A mediates fast axonal transport of membranous vesicles including

308   synaptic vesicle precursors and dense core vesicles, and is critical in synaptogenesis (17, 18). In

309   differentiated PC12 cells, KIF1A protein levels decreased rapidly upon treatment with the protein

310   synthesis inhibitor cycloheximide (CHX), and showed an apparent half-life of approximately 4

311   hours. The half-lives of kinesin-1 and -2 motors were longer under the same condition (>8 hours).

312   Our results are consistent with a previous proteomics study using rat cortical neurons, where

313   KIF1A had the 8th shortest half-life in among ~2800 proteins measured ($t_{1/2}$ = 0.42 day) (32),

314   suggesting that this is a consistent characteristic of KIF1A in both CNS and PNS neurons. The

315   decline in KIF1A concentration is blocked when PC12 cells were treated simultaneously with

316   CHX and MG132, demonstrating that the loss of KIF1A protein was predominately mediated by

317   proteasomes. Our results confirmed another previous proteomics study where the half-life of the

318   KIF1A protein increased and the degradation rate dropped upon inhibition of proteasomes (33).

319

320   UNC-104, the KIF1A homolog in *C. elegans*, was shown to be degraded at synapse regions *in vivo*

321   in an ubiquitin-dependent manner. Moreover, the stability of the motor was linked to its capacity

15

322   for cargo binding (22). It was also proposed that the degradation of Liprinα1, an cargo adaptor for

323   KIF1A, by either proteasome or CaMKII phosphorylation was required for the "unloading" of

324   LAR (leukocyte common antigen- related) family of receptor protein tyrosine phosphatases at

325   synapses (34, 35). These studies imply a potential mechanistic link between motor degradation

326   and cargo release. Since we also observed proteasomal degradation of KIF1A in fluidically and

327   physically separated axons during PRV infection, KIF1A may be actively degraded in axons by

328   proteasomes upon release of viral cargo.

329

330   The relative stabilities of KIF5 and KIF3A proteins were unexpected, since several lines of

331   evidence suggested that both motors are actively degraded in axons (36-39). However, unlike

332   KIF1A, both KIF5 and KIF3A also mediate short distance transport of cellular cargoes within cell

333   bodies, and may be recycled for future use. The particular short half-life of KIF1A is consistent

334   with the idea that KIF1A is a specialized motor for axonal transport.

335

336   **The reduction of KIF1A mRNA upon PRV infection.**

337

338   The dynamic steady state level of KIF1A protein in uninfected cells suggests that, in PRV-infected

339   cells, KIF1A protein concentration may be sensitive to viral host shutoff or mRNA instability

340   induced by infection. Alphaherpesviruses reduce/block the synthesis of some cellular proteins after

341   infection to facilitate viral gene expression and to evade host antiviral responses. The virion host

342   shutoff protein (vhs) is an endoribonuclease encoded by the viral UL41 gene (40-42). HSV-1 vhs

343   enters the infected cells as a part of incoming virion tegument, and subsequently interacts with

344   translation initiation factors eIF4H, eIF4B, and eIF4A to degrade host mRNAs and halts host

16

345 protein translation (43, 44). Infection of PC12 cells with inactivated virions (UV'd, IE180-null

346 PRV) did not lead to the decline in KIF1A protein. We conclude that tegument proteins like vhs

347 delivered by entering particles are not sufficient for the reduction in KIF1A protein during

348 infection.

349

350 We further analyzed the accumulation of cellular mRNAs during infection and compared the levels

351 of kinesin motor transcripts. qRT-PCR analysis of PRV-infected PC12 cells revealed that the

352 levels of KIF1A, KIF5B, and GAPDH transcripts all decreased significantly at similar rates,

353 starting as early as 3 h.p.i., and reaching almost full depletion at 12 h.p.i. The reduction of KIF1A

354 mRNA reduced the rate of new protein synthesis. This reduction of new KIF1A proteins, coupled

355 with the active degradation of existing KIF1A motors by proteasomes, leads to the significant

356 decrease in KIF1A protein concentration in infected neuronal cells.

357

358 **The PRV anterograde sorting complex US9/gE/gI directs more KIF1A motors to be**

359 **degraded by proteasomes.**

360

361 US9 forms a complex with two other membrane proteins, gE and gI to sort progeny PRV virions

362 in transport vesicles into axons (14, 15)(J. Scherer, I. B. Hogue, Z. A. Yaffe, N. S. Tanneti, B. Y.

363 Winer, M. Vershinin, L. W. Enquist, submitted for publication). We have previously identified

364 KIF1A as an interaction partner of PRV US9 protein (14). In addition, we had noted that two

365 ubiquitin ligases, NEDD4 and viral EP0, co-purified with US9 and KIF1A (14). Since we also

366 showed accelerated proteasomal degradation of KIF1A during infection, we hypothesized that the

367 PRV anterograde sorting complex, gE/gI/US9, could independently recruit KIF1A to viral

17

368   transport vesicles for axonal sorting and transport, and eventually promote the proteasomal

369   degradation of KIF1A in axons. We investigated this hypothesis using adenovirus vectors to

370   express the components of the anterograde sorting complex (one by one and in combination) in

371   neuronal cells without PRV infection. In cells transduced with adenovirus vectors expressing US9,

372   gE, and gI, US9 interacts with the gE/gI heterodimer in lipid rafts, and the US9, gE, and gI complex

373   was observed to undergo axonal anterograde transport together with long-range motility

374   characteristic of anterogradely-moving PRV virions in axons (J. Scherer, I. B. Hogue, Z. A. Yaffe,

375   N. S. Tanneti, B. Y. Winer, M. Vershinin, L. W. Enquist, submitted for publication). PRV envelope

376   proteins, US9/gE/gI, when expressed together in neuronal cells, induced a significant decline in

377   KIF1A protein concentration. Therefore we concluded that the viral anterograde sorting complex

378   US9/gE/gI promotes the accelerated loss of KIF1A proteins.

379

380   This result is consistent with experiments where PC12 cells were infected with PRV strains that

381   fail to express a functional US9/gE/gI complex to recruit KIF1A to undergo anterograde spread.

382   These PRV mutants still promote host shutoff, leading to the decline of KIF1A proteins late in

383   infection. However, the rate of decline is slower than that observed after wildtype PRV infection,

384   suggesting that the US9/gE/gI complex accelerates the degradation of KIF1A by the proteasomes.

385   The inhibition of late gene expression (e.g. US9) by AraT treatment also led to a minor yet

386   statistically significant stabilization of KIF1A protein concentration. We concluded that the PRV

387   anterograde sorting complex US9/gE/gI directs more KIF1A motors to be degraded by

388   proteasomes. This might shed light on the mechanisms underlying the intrinsic instability of

389   KIF1A protein, which potentially stem from the interaction of the motor with its cellular cargoes.

390

18

391 **PRV infection induces the accelerated loss of KIF1A protein through two separate**

392 **mechanisms.**

393

394 Our model to account for our results is shown in Figure 8. KIF1A motors, mediating the

395 anterograde transport of the vesicles in axons critical for synapse formation and function, are

396 inherently prone to proteasomal degradation. Such intrinsic instability results in the dynamic

397 steady state level of KIF1A protein maintained through rapid protein synthesis and proteasomal

398 degradation in neuronal cells (Fig. 8A). The balance between protein synthesis and degradation is

399 disrupted by PRV infection through two separate mechanisms (Fig. 8B). First, PRV infection

400 promotes the nonspecific loss of KIF1A mRNAs, and reduces the synthesis of KIF1A protein. The

401 concentration of existing KIF1A protein continues to decline through default proteasomal

402 degradation. Second, PRV infection accelerates the degradation of KIF1A protein through the

403 PRV anterograde sorting complex US9/gE/gI. We propose that US9 recruits KIF1A to transport

404 vesicles containing enveloped virions or light particles, as well as vesicles with viral glycoproteins

405 for axonal sorting and transport, and eventually this complex promotes the proteasomal

406 degradation of KIF1A in axons.

407

408 Our work implies that after reactivation from latently infected PNS neurons, the targeted loss of

409 KIF1A motor proteins leads to a limited time window for sorting into and transport of viral

410 particles in axons for further host-to-host spread. Indeed, the loss of available KIF1A motors over

411 the course of PRV infection results in reduced recruitment of the motor by US9 (14). While our

412 work has focused on PRV, it would be important to know if infection by other alphaherpesviruses

413 promotes differential degradation of axonal motor proteins. The anterograde transport of HSV-1

19

414   has been shown to be mediated by kinesin-1 (KIF5A, KIF5B, and KIF5C) and kinesin-3 (KIF1A)

415   motors (11, 45)(E. Engel and L.W. Enquist, unpublished data).   It is therefore of clinical

416   importance to determine if HSV-1 infection induces similar loss in human neurons *in vitro*. Such

417   a loss of kinesin-1 and kinesin-3 motors after reactivation from PNS neuron could have significant

418   consequence for long term neuronal function. Further work is required to understand whether PNS

419   neurons can tolerate the loss of specific kinesin motors during reactivation episodes, and whether

420   the motor concentrations are restored after reactivation if those neurons survive.

421

422   **Materials and Methods:**

423

424   **Cell lines and viruses.** Porcine kidney epithelial cells (PK15, ATCC) were maintained in

425   Dulbecco modified Eagle medium (DMEM, Hyclone) supplemented with 10% fetal bovine serum

426   (FBS, Hyclone) and 1% penicillin-streptomycin (Hyclone). PK15 cells were used to propagate and

427   determine titers of all PRV strains used in this study. 293A cells (Invitrogen) were used to

428   propagate and determine the titer of adenovirus vectors used in this study. The neuronal PC12 cell

429   line has been used extensively to model primary neurons infection of PRV and to reproduce the

430   US9-associated transport phenotype (14, 46). PC12 cells were cultured on dishes coated with type

431   1 rat tail collagen (BD Bioscience, Bedford, MA) in 85% RPMI 1640 (Thermo Fisher)

432   supplemented with 10% horse serum(Life Technologies) and 5% FBS (47). PC12 cells were

433   differentiated in RPMI 1640 supplemented with 1% horse serum and nerve growth factor (NGF,

434   2,5S, Invitrogen) at 100 ng/ml (47). Differentiation medium was replaced every third day for eight

435   days before infection.

436

437   The PRV viral strains used in this study include both wild-type laboratory stain and recombinants.

438   PRV Becker is a wildtype strain (25, 26). PRV Bartha is an attenuated vaccine strain (48, 49). PRV

439   BaBe is a viral recombinant in the PRV Becker background with deletions from the unique short

440   (US) region of PRV Bartha (50). HKO146 lacks the only PRV immediate early gene IE180 and

441   expresses hSyn Cre-t2a-venus in US9 loci in the PRV Becker background (H. Oyibo, P.

442   Znamenskiy, H. V. Oviedo, L. W. Enquist, A. Zador, unpublished data). PRV161 harbors a

443   complete deletion of the US9 gene in the PRV Becker background (51). PRV172 harbors two

444   tyrosine to alanine substitutions (Y49 Y50 to AA) in the PRV Becker background (30). Individual

445   replication-deficient adenovirus vectors expressing GFP, GFP-US9, gE-mCherry, gI-mTurquoise

446   2 were previously reported (14, 52).

447

448   **Primary neuronal culture.** Embryonic superior cervical ganglia (SCG) neurons were isolated and

449   cultured as previously described (53). Briefly, superior cervical ganglia (SCG) were isolated from

450   day 17 Sprague-Dawley rat (Hilltop Labs) embryos, plated and maintained on poly-DL-ornithine

451   (Sigma-Aldrich) and laminin (Invitrogen) coated dishes (Falcon or MatTek) in neuronal medium

452   made with neurobasal medium (Gibco) supplemented with 1% penicillin-streptomycin with 2 mM

453   glutamine (Invitrogen), 2% B-27 (Gibco), and 100 ng/ml neuronal growth factor (NGF, 2.5S

454   (Invitrogen)). On two days post plating, 1 mM cytosine-D-arabinofuranoside (AraC; Sigma-

455   Aldrich) was added to selectively eliminate dividing non-neuronal cells in culture for two days.

456   SCG neurons were allowed to differentiate for at least 14 days before infection.

457

458   Compartmented neuronal cultures were prepared on poly-ornithine and laminin coated plastic

459   dishes. Parallel grooves were etched into the plastic dish, and 1% methylcellulose in neuronal

21

460   medium was added to the region that would underlie the middle compartment of the isolator rings.

461   CAMP320 isolator rings (Tyler Research) were coated with autoclaved silicone vacuum grease on

462   one side and gently applied to the dish so that the etched grooves extended across three

463   compartments. Dissociated SCG neurons were plated in the soma compartment (S), and were

464   allowed to extend axons along the grooves through the M compartment and into the neurite (N)

465   compartment for 14-28 days.

466

467   **Viral infection in neuronal culture.** Triplicates of differentiated PC12 cells were infected with

468   the indicated PRV strain at a multiplicity of infection (MOI) of 20 at the indicated hours post

469   infection. Infected cells from each triplicate were harvested and combined into a single sample for

470   further biochemical analysis. Compartmented SCG neuronal cultures were infected in the soma (S)

471   compartment for 24 hours. Neuronal cell bodies from the S compartments and axons from the N

472   compartments were harvested for biochemical analysis. The proteasome inhibitor MG132

473   (Millipore Sigma) was prepared in DMSO and added at a concentration of 2.5 μM. The herpesvirus

474   DNA replication inhibitor thymine 1-β-D-arabinofuranoside (AraT) (Millipore Sigma) was added

475   at a concentration of 100μg/ml 15 minutes prior to infection.

476

477   **Adenovirus vectors transduction.** The adenovirus vectors expressing GFP, GFP-US9, gE-

478   mCherry, and gI-mTurquoise-2 were reported previously (14, 52). Adenovirus vectors were

479   propagated in 293A cells, and cell-associated virus was harvested in serum-free DMEM media.

480   Adenoviral transduction of differentiated PC12 cells was performed for up to five days to ensure

481   the expression of fluorescent transgene(s) in the majority of cells (>90%).

482

22

483   **Quantitative Western blotting analysis.** Neuronal cell lysates were prepared in

484   radioimmunoprecipitation assay buffer (RIPA) (50mM Tris-HCl, 150mM NaCl, 5mM EDTA, 1%

485   NP-40, 0.1% SDS, 0.1% Triton X-100, and 1% sodium deoxycholate, pH 8.0) supplemented with

486   1 mM dithiothreitol (DTT, Sigma-Aldrich) and protease inhibitor cocktail (Sigma-Aldrich). Cell

487   lysates were kept on ice for one hour and centrifuged at 13,200 rpm at 4°C for 10 minutes. Cleared

488   cell lysates were transferred to a new tube and mixed with 4X LDS sample loading buffer

489   (Invitrogen) supplemented with 240 mM DTT. The samples were heated at 95°C for 10 minutes

490   and centrifuged at 4°C for 10 minutes to remove potential protein aggregates before proteins were

491   separated in gradient polyacrylamide gels (4-12%) (Invitrogen). Proteins were transferred onto

492   nitrocellulose membranes (Whatman) by semidry transfer (Bio-Rad). Membranes were blocked in

493   5% nonfat dry milk in Tris buffer saline with 0.1% Tween 20 (TBS-T) for 1 hour at room

494   temperature. Primary and secondary antibodies for immunoblot analysis were prepared in 1% milk

495   in TBS-T. Protein bands were imaged by LI-COR Odyssey CLx imaging system. The signal

496   intensity was quantified using LI-COR Image Studio Lite software.

497

498   Antibodies used in this study included a mouse monoclonal KIF1A antibody (Clone 16, BD, at

499   1:2000), a mouse monoclonal kinesin heavy chain antibody (MAB-1614, Millipore Sigma, at

500   1:1000), a mouse monoclonal KIF3A antibody (Clone K2.4, Covance Inc., at 1:1000), a mouse

501   monoclonal β-Actin antibody (Sigma, at 1:10000), a monoclonal US9 antibody (IA8, DSHB, at

502   1:100), a rabbit polyclonal GST-EP0 antibody at 1:2000 (54), a mouse monoclonal PRV VP5

503   antibody at 1:1000 (55), a mouse monoclonal PRV US3 antibody at 1:10000 (56), a rabbit

504   polyclonal gE cytoplasmic tail antibody at 1:1000 (57), a rabbit polyclonal gI antibody, a generous

505   gift from K. Bienkowska-Szewczyk, at 1:1000 (58). IRDye secondary antibodies included 800CW

506   donkey anti-mouse IgG, 800CW donkey anti-rabbit IgG, and 680RD donkey anti-rabbit at 1:15000

507   (LI-COR).

508

509   **qRT-PCR analysis.** Differentiated PC12 cells infected with PRV were harvested and subjected to

510   total RNA extraction using an RNeasy Plus Mini Kit (Qiagen). First strand cDNA synthesis of

511   isolated RNAs was performed with SuperScript III First Strand synthesis kit with Oligo (dT)

512   primer (Invitrogen). Quantitative reverse transcription PCR was performed using Eppendorf

513   Realplex^2 Mastercycler with reaction mixtures prepared with KAPA SYBR Fast Universal qPCR

514   Kit (KAPA Biosystems). The PCR primers for KIF1A, KIF5B, GAPDH, and 18s rRNA were

515   reported elsewhere (59). The qRT-PCR reaction samples were prepared in triplicates. The relative

516   abundance of RNA in each sample was calculated using the $-\Delta\Delta C_T$ method normalized to 18s

517   rRNA and subsequently to uninfected samples.

518

519   **Statistical analysis.** One-way analysis of variance (ANOVA) with Tukey's posttest, and two-way

520   ANOVA with Sidak's posttest were performed using GraphPad Prism 6. Values in text, graphs,

521   and figure legends throughout the manuscript are means ± standard errors of the means (SEM).

522

523   **Image production.**

524   Cartoon illustrations were made with web application BioRender under Princeton University

525   license for education use.

526

527   **Ethics Statement.** All animal work was performed in accordance with the Princeton Institutional

528   Animal Care and Use Committee (protocols 1947-16). Princeton personnel are required to adhere

24

529   to applicable federal, state, local and institutional laws and policies governing animal research,

530   including the Animal Welfare Act and Regulations (AWA); the Public Health Service Policy on

531   Humane Care and Use of Laboratory Animals; the Principles for the Utilization and Care of

532   Vertebrate Animals Used in Testing, Research and Training; and the Health Research Extension

533   Act of 1985.

534

535   **Acknowledgement**

540

541   **References**

542   1.   Steiner I, Kennedy PGE, Pachner AR. 2007. The neurotropic herpes viruses: herpes

543   simplex and varicella-zoster. The Lancet Neurology 6:1015-1028.

544   2.   Koelle DM, Corey L. 2008. Herpes simplex: insights on pathogenesis and possible

545   vaccines. Annu Rev Med 59:381-95.

546   3.   Pomeranz LE, Reynolds AE, Hengartner CJ. 2005. Molecular biology of pseudorabies

547   virus: impact on neurovirology and veterinary medicine. Microbiol Mol Biol Rev 69:462-

548   500.

549   4.   Smith G. 2012. Herpesvirus transport to the nervous system and back again. Annu Rev

550   Microbiol 66:153-76.

551 5.   Hirokawa N, Noda Y, Tanaka Y, Niwa S. 2009. Kinesin superfamily motor proteins and

552   intracellular transport. Nat Rev Mol Cell Biol 10:682-96.

553 6.   Hirokawa N, Niwa S, Tanaka Y. 2010. Molecular motors in neurons: transport mechanisms

554   and roles in brain function, development, and disease. Neuron 68:610-38.

555 7.   Gluska S, Zahavi EE, Chein M, Gradus T, Bauer A, Finke S, Perlson E. 2014. Rabies Virus

556   Hijacks and accelerates the p75NTR retrograde axonal transport machinery. PLoS Pathog

557   10:e1004348.

558 8.   Smith GA, Pomeranz L, Gross SP, Enquist LW. 2004. Local modulation of plus-end

559   transport targets herpesvirus entry and egress in sensory axons. Proc Natl Acad Sci U S A

560   101:16034-9.

561 9.   Zaichick SV, Bohannon KP, Hughes A, Sollars PJ, Pickard GE, Smith GA. 2013. The

562   herpesvirus VP1/2 protein is an effector of dynein-mediated capsid transport and

563   neuroinvasion. Cell Host Microbe 13:193-203.

564 10. Buch A, Muller O, Ivanova L, Dohner K, Bialy D, Bosse JB, Pohlmann A, Binz A,

565   Hegemann M, Nagel CH, Koltzenburg M, Viejo-Borbolla A, Rosenhahn B, Bauerfeind R,

566   Sodeik B. 2017. Inner tegument proteins of Herpes Simplex Virus are sufficient for

567   intracellular capsid motility in neurons but not for axonal targeting. PLoS Pathog

568   13:e1006813.

569 11. DuRaine G, Wisner TW, Paul Howard P, Johnson DC. 2018. Kinesin-1 Proteins KIF5A, -

570   5B, and -5C Promote Anterograde Transport of Herpes Simplex Virus Enveloped Virions

571   in Axons. Journal of Virology 92.

572   12.   Radtke K, Kieneke D, Wolfstein A, Michael K, Steffen W, Scholz T, Karger A, Sodeik B.

573   2010. Plus- and minus-end directed microtubule motors bind simultaneously to herpes

574   simplex virus capsids using different inner tegument structures. PLoS Pathog 6:e1000991.

575   13.   Wolfstein A, Nagel CH, Radtke K, Dohner K, Allan VJ, Sodeik B. 2006. The inner

576   tegument promotes herpes simplex virus capsid motility along microtubules in vitro.

577   Traffic 7:227-37.

578   14.   Kramer T, Greco TM, Taylor MP, Ambrosini AE, Cristea IM, Enquist LW. 2012. Kinesin-

579   3 mediates axonal sorting and directional transport of alphaherpesvirus particles in neurons.

580   Cell Host Microbe 12:806-14.

581   15.   Kratchmarov R, Kramer T, Greco TM, Taylor MP, Ch'ng TH, Cristea IM, Enquist LW.

582   2013. Glycoproteins gE and gI are required for efficient KIF1A-dependent anterograde

583   axonal transport of alphaherpesvirus particles in neurons. J Virol 87:9431-40.

584   16.   Scherer J, Yaffe ZA, Vershinin M, Enquist LW. 2016. Dual-Color Herpesvirus Capsids

585   Discriminate Inoculum from Progeny and Reveal Axonal Transport Dynamics. J Virol

586   90:9997-10006.

587   17.   Siddiqui N, Straube A. 2017. Intracellular Cargo Transport by Kinesin-3 Motors.

588   Biochemistry (Mosc) 82:803-815.

589   18.   Kern JV, Zhang YV, Kramer S, Brenman JE, Rasse TM. 2013. The kinesin-3, unc-104

590   regulates dendrite morphogenesis and synaptic development in Drosophila. Genetics

591   195:59-72.

592   19.   Klopfenstein DR, Tomishige M, Stuurman N, Vale RD. 2002. Role of

593   Phosphatidylinositol(4,5)bisphosphate Organization in Membrane Transport by the

594   Unc104 Kinesin Motor. Cell 109:347-58.

595   20.   Yonekawa Y, Harada A, Okada Y, Funakoshi T, Kanai Y, Takei Y, Terada S, Noda T,

596   Hirokawa N. 1998. Defect in Synaptic Vesicle Precursor Transport and Neuronal Cell

597   Death in KIF1A Motor Protein–deficient Mice. The Journal of Cell Biology 141:431-441.

598   21.   Okada Y, Yamazaki H, Sekine-Aizawa Y, Hirokawa N. 1995. The Neuron-Specific

599   Kinesin Superfamily Protein KIFIA Is a Unique Monomeric Motor for Anterograde

600   Axonal Transport of Synaptic Vesicle Precursors. Cell 81:769-780.

601   22.   Kumar J, Choudhary BC, Metpally R, Zheng Q, Nonet ML, Ramanathan S, Klopfenstein

602   DR, Koushika SP. 2010. The Caenorhabditis elegans Kinesin-3 motor UNC-104/KIF1A is

603   degraded upon loss of specific binding to cargo. PLoS Genet 6:e1001200.

604   23.   Smith GA, Gross SP, Enquist LW. 2001. Herpesviruses use bidirectional fast-axonal

605   transport to spread in sensory neurons. Proc Natl Acad Sci U S A 98:3466-70.

606   24.   Becker Y, Tavor E, Asher Y, Berkowitz C, Moyal M. 1993. Effect of Herpes Simplex

607   Virus Type-1 UL41 Gene on the Stability of mRNA from the Cellular Genes: beta-actin,

608   Fibronectin, Glucose Transporter-l, and Docking Protein, and on Virus Intraperitoneal

609   Pathogenicity to Newborn Mice. Virus Genes 7:133-143.

610   25.   Smibert CA, Johnson DC, Smiley JR. 1992. Identification and characterization of the

611   virion-induced host shutoff product of herpes simplex virus gene UL41. Journal of General

612   Virology 73:467-470.

613   26.   Hardy WR, Sandri-Goldin RM. 1994. Herpes Simplex Virus Inhibits Host Cell Splicing,

614   and Regulatory Protein ICP27 Is Required for This Effect. Journal of Virology 68:7790-

615   7799.

616   27.   Hardwicke MA, Sandri-Goldin RM. 1994. The Herpes Simplex Virus Regulatory Protein
617   ICP27 Contributes to the Decrease in Cellular mRNA Levels during Infection. Journal of
618   Virology 68:4797-4810.

619   28.   Wu BW, Engel EA, Enquist LW. 2014. Characterization of a replication-incompetent
620   pseudorabies virus mutant lacking the sole immediate early gene IE180. MBio 5:e01850.

621   29.   Oyibo HK, Znamenskiy P, Oviedo HV, Enquist LW, Zador AM. 2014. Long-term Cre-
622   mediated retrograde tagging of neurons using a novel recombinant pseudorabies virus.
623   Front Neuroanat 8:86.

624   30.   Brideau A, D., Eldridge M, Enquist LW. 2000. Directional Transneuronal Infection by
625   Pseudorabies Virus Is Dependent on an Acidic Internalization Motif in the Us9
626   Cytoplasmic Tail. Journal of Virology 74:4549-4561.

627   31.   Taylor MP, Kramer T, Lyman MG, Kratchmarov R, Enquist LW. 2012. Visualization of
628   an alphaherpesvirus membrane protein that is essential for anterograde axonal spread of
629   infection in neurons. MBio 3.

630   32.   Cohen LD, Zuchman R, Sorokina O, Muller A, Dieterich DC, Armstrong JD, Ziv T, Ziv
631   NE. 2013. Metabolic turnover of synaptic proteins: kinetics, interdependencies and
632   implications for synaptic maintenance. PLoS One 8:e63191.

633   33.   Hakim V, Cohen LD, Zuchman R, Ziv T, Ziv NE. 2016. The effects of proteasomal
634   inhibition on synaptic proteostasis. EMBO J 35:2238-2262.

635   34.   Hoogenraad CC, Feliu-Mojer MI, Spangler SA, Milstein AD, Dunah AW, Hung AY,
636   Sheng M. 2007. Liprinalpha1 degradation by calcium/calmodulin-dependent protein
637   kinase II regulates LAR receptor tyrosine phosphatase distribution and dendrite
638   development. Dev Cell 12:587-602.

639   35.   Schlager MA, Hoogenraad CC. 2009. Basic mechanisms for recognition and transport of

640   synaptic cargos. Mol Brain 2:25.

641   36.   Kondo S, Sato-Yoshilake R, Noda Y, Aizawa H, Nakata T, Matsuura Y, Hirokawa N. 1994.

642   KIF3A Is a New Microtubule-based Anterograde Motor in the Nerve Axon. The Journal

643   of Cell Biology 125:1095-1107.

644   37.   Yamazaki H, Nakata T, Okada Y, Hirokawa N. 1995. KIF3A/B: A Heterodimeric Kinesin

645   Superfamily Protein That Works as a Microtubule Plus End-directed Motor for Membrane

646   Organelle Transport. The Journal of Cell Biology 130:1387-1399.

647   38.   Li J-Y, Pfister KK, Brady S, Dahlstrom A. 1999. Axonal Transport and Distribution of

648   Immunologically Distinct Kinesin Heavy Chains in Rat Neurons. Journal of Neuroscience

649   Research 58.

650   39.   Hirokawa N, SatoYoshitake R, Kobayashi N, Pfister KK, Bloom GS, Brady ST. 1991.

651   Kinesin Associates with Anterogradely Transported Membranous Organelles In Vivo. The

652   Journal of Cell Biology, 114:295-302.

653   40.   Everly DN, Jr., Feng P, Mian IS, Read GS. 2002. mRNA degradation by the virion host

654   shutoff (Vhs) protein of herpes simplex virus: genetic and biochemical evidence that Vhs

655   is a nuclease. J Virol 76:8560-71.

656   41.   Perez-Parada J, Saffran HA, Smiley JR. 2004. RNA degradation induced by the herpes

657   simplex virus vhs protein proceeds 5' to 3' in vitro. J Virol 78:13391-4.

658   42.   Taddeo B, Roizman B. 2006. The virion host shutoff protein (UL41) of herpes simplex

659   virus 1 is an endoribonuclease with a substrate specificity similar to that of RNase A. J

660   Virol 80:9341-5.

661   43.   Doepker RC, Hsu WL, Saffran HA, Smiley JR. 2004. Herpes simplex virus virion host
662   shutoff protein is stimulated by translation initiation factors eIF4B and eIF4H. J Virol
663   78:4684-99.
664   44.   Feng P, Everly DN, Jr., Read GS. 2005. mRNA decay during herpes simplex virus (HSV)
665   infections: protein-protein interactions involving the HSV virion host shutoff protein and
666   translation factors eIF4H and eIF4A. J Virol 79:9651-64.
667   45.   Diefenbach RJ, Davis A, Miranda-Saksena M, Fernandez MA, Kelly BJ, Jones CA, LaVail
668   JH, Xue J, Lai J, Cunningham AL. 2016. The Basic Domain of Herpes Simplex Virus 1
669   pUS9 Recruits Kinesin-1 To Facilitate Egress from Neurons. J Virol 90:2102-11.
670   46.   Lyman MG, Curanovic D, Enquist LW. 2008. Targeting of pseudorabies virus structural
671   proteins to axons requires association of the viral Us9 protein with lipid rafts. PLoS Pathog
672   4:e1000065.
673   47.   Ch'ng TH, Flood EA, Enquist LW. 2005. Culturing Primary and Transformed Neuronal
674   Cells for Studying Pseudorabies Virus Infection. Methods Mol Biol 292:299-316.
675   48.   Platt KB, Mare CJ, Hinz PN. 1979. Differentiation of Vaecine Strains and Field Isolates of
676   Pseudorabies (Aujeszky's Disease) Virus: Thermal Sensitivity and Rabbit Virulence
677   Markers. Archives of Virology 60:13-23.
678   49.   Szpara ML, Tafuri YR, Parsons L, Shamim SR, Verstrepen KJ, Legendre M, Enquist LW.
679   2011. A wide extent of inter-strain diversity in virulent and vaccine strains of
680   alphaherpesviruses. PLoS Pathog 7:e1002282.
681   50.   Card JP, Whealy ME, Robbins AK, Enquist LW. 1992. Pseudorabies Virus Envelope
682   Glycoprotein gI Influences both Neurotropism and Virulence during Infection of the Rat
683   Visual System. Journal of Virology 66:3032-3041.

31

684   51.   Brideau AD, Card JP, Enquist LW. 2000. Role of pseudorabies virus Us9, a type II

685   membrane protein, in infection of tissue culture cells and the rat nervous system. J Virol

686   74:834-45.

687   52.   Hogue IB, Scherer J, Enquist LW. 2016. Exocytosis of Alphaherpesvirus Virions, Light

688   Particles, and Glycoproteins Uses Constitutive Secretory Mechanisms. MBio 7.

689   53.   Curanovic D, Ch'ng TH, Szpara M, Enquist L. 2009. Compartmented neuron cultures for

690   directional infection by alpha herpesviruses. Curr Protoc Cell Biol Chapter 26:Unit 26 4.

691   54.   Brukman A, Enquist LW. 2006. Pseudorabies virus EP0 protein counteracts an interferon-

692   induced antiviral state in a species-specific manner. J Virol 80:10871-3.

693   55.   Lyman MG, Feierbach B, Curanovic D, Bisher M, Enquist LW. 2007. Pseudorabies virus

694   Us9 directs axonal sorting of viral capsids. J Virol 81:11363-71.

695   56.   Olsen LM, Ch'ng TH, Card JP, Enquist LW. 2006. Role of pseudorabies virus Us3 protein

696   kinase during neuronal infection. J Virol 80:6387-98.

697   57.   Tirabassi RS, Enquist LW. 2000. Role of the Pseudorabies Virus gI Cytoplasmic Domain

698   in Neuroinvasion, Virulence, and Posttranslational N-Linked Glycosylation. Journal of

699   Virology 74:3505–3516.

700   58.   Tirabassi RS, Enquist LW. 1998. Role of Envelope Protein gE Endocytosis in the

701   Pseudorabies Virus Life Cycle. Journal of Virology 72:4571–4579.

702   59.   Baptista FI, Pinto MJ, Elvas F, Almeida RD, Ambrosio AF. 2013. Diabetes alters KIF1A

703   and KIF5B motor proteins in the hippocampus. PLoS One 8:e65515.

704   **Figure legends**

705   **Fig. 1. KIF1A protein undergoes rapid accumulation and degradation in neuronal cells upon**

706   **MG132 and CHX treatments.**

32

707   (A) Differentiated PC12 cells were treated with the translation inhibitor cycloheximide,

708   proteasome inhibitor MG132, or both cycloheximide and MG132 for 2, 4, 6, 8, hours. Cells were

709   harvested at indicated time points and lysates were analyzed by Western blot to monitor protein

710   levels of KIF1A, KIF5, KIF3A, and actin. (B-D) KIF1A, KIF5, and KIF3A protein levels were

711   measured by band intensities and normalized to actin protein levels for each time interval.

712   Normalized values were again normalized to that of Mock 0 hour samples. Values are means plus

713   SEMs (error bar) from three independent experiments. n.s., not statistically significant, **, $P<0.01$,

714   ***, $P<0.001$, ****, $P<0.0001$ for the indicated comparison at 8 hours post treatment.

715

716   **Fig. 2. KIF1A protein concentration is reduced during PRV infection in neuronal cells.**

717   (A and B) Differentiated PC12 cells were mock-infected or infected with PRV Becker for 3, 8, 12,

718   16, 20, 24 hours with MOI of 20. Cells were harvested at the time intervals shown, and lysates

719   were analyzed by Western blot to monitor protein levels of KIF1A, KIF5, KIF3A, and actin.

720   Kinesin levels were measured by band intensities and normalized with respect to actin levels at

721   each time interval. Normalized values were again normalized to that of Mock 0 hour samples.

722   Values are means plus SEMs (error bars) from four independent experiments. n.s., not statistically

723   significant, ***, $P<0.001$, ****, $P<0.0001$.

724

725   **Fig. 3. The abundance of KIF1A, KIF5B, and GAPDH transcripts is significantly reduced in**

726   **PRV-infected neuronal cells.**

727   Differentiated PC12 cells were infected with (A) PRV Becker or (B) PRV Bartha for 3, 8, 12, 16,

728   20, 24 hours with MOI of 20. Cells were harvested at the time intervals shown. Total RNA were

729   extracted and qRT-PCR quantification was performed to measure KIF1A, KIF5B, and GAPDH

730   mRNA levels using 18S rRNA as internal control at each time interval. The normalized values are

731   then normalized to that of Mock 0 hour samples. Values are means plus SEMs (error bars) from

732   three independent experiments.

733

734   **Fig. 4. KIF1A is degraded by the proteasome in the late phase of PRV infection.**

735   Differentiated PC12 cells were (A) mock-infected or (B) infected with PRV Becker for 8, 12, 16,

736   20, 24 hours with MOI of 20. In a parallel experiment, the proteasomal inhibitor, MG132, was

737   added at 12 hours post infection at the concentration of 2.5 μM. KIF1A levels were analyzed by

738   Western blot and normalized to actin levels at each time interval. Normalized values were again

739   normalized to that of Mock 0 hour samples. Values are means plus SEMs (error bars) from three

740   independent experiments. **, $P<0.01$ for comparison between PRV-infected and PRV-

741   infected+MG132 samples.

742

743   **Fig. 5. PRV infection of compartmented primary neuronal cultures leads to reduction of**

744   **KIF1A protein and proteasomal degradation in axons.**

745   (A) Illustration of *in vitro* culture of primary superior cervical ganglion neurons using modified

746   Campenot chambers that include the S (soma), M (methocel), and N (neurite, axon termini)

747   compartments. 10^6 PFU of PRV Becker was added in the S (soma) compartment. (B and C) SCG

748   neurons were infected at the Soma (S) compartment with PRV Becker for 24 hours. (B) Cell bodies

749   and axons from S and N compartments were collected at the time intervals show, and lysate were

750   analyzed by Western blot to monitor the levels of KIF1A and Actin. (C) DMSO or MG132 (2.5

751   μM) were added to the N (Neurite) compartment at 8 hpi. Cell bodies and axons from S and N

752   compartments were collected at the time intervals show, and lysate were analyzed by Western blot

753   to monitor the levels of KIF1A and Actin.

754

755   **Fig. 6. Accelerated proteasomal degradation of KIF1A during infection requires the**

756   **expression of both PRV early and late proteins**.

757   (A) *De novo* PRV viral protein synthesis is required for KIF1A degradation. Differentiated PC12

758   cells were mock-infected or infected with PRV Becker, UV'd PRV Becker, or IE180-null PRV

759   (HKO146) for 24 hours with MOI of 20. Cells were harvested and lysates were analyzed by

760   Western blot to monitor the levels of KIF1A, actin, and VP5 at indicated time intervals. (B)

761   Differentiated PC12 cells were mock-treated or treated with AraT (100μg/ml) starting 15 minutes

762   before being infected with PRV Becker for 0, 8, 12, 16, 20, 24 hours. Samples were collected at

763   the indicated time intervals. Lysates were subjected to Western Blot analysis to measure protein

764   levels of KIF1A, actin, VP5, and EP0. (C) For every infection, KIF1A protein abundance were

765   measured by band intensities and normalized with respect to actin levels at each time interval.

766   Normalized values were then normalized to that for Mock 0 hour samples. Values are means plus

767   SEMs (error bars) from three independent experiments. *, P<0.05 for PRV Becker vs. PRV Becker

768   with AraT comparison at specified time interval.

769

770   **Fig. 7. PRV anterograde-spread complex US9/gE/gI promotes the accerlated degradation of**

771   **KIF1A proteins.**

772   (A) Differentiated PC12 cells were infected with PRV Becker, or different PRV mutants defective

773   in anterograde spread (results from PRV BaBe and PRV161 infections are shown) for 0, 8, 12, 16,

774   20 ,24 hours. Cells were harvested and lysates were analyzed by Western blot to monitor KIF1A

35

775   and actin protein Level. (B) For every infection, KIF1A levels were measured by band intensities

776   and normalized with respect to actin levels at each time interval. Normalized values were then

777   normalized to that for Mock 0 hour samples. Values are means plus SEMs (error bars) from seven

778   independent experiments. *, P<0.05 for all mutants vs. PRV Becker at specified time interval. (C)

779   Differentiated PC12 cells were transduced with Adenoviral vectors expressing GFP, GFP-US9, or

780   GFP-US9/gE-mCherry/gI-mTurquoise 2. Cells were collected at indicated days post transduction

781   (d.p.t.) and subjected to Western Blot Analysis to monitor KIF1A and Actin level.

782

783   **Fig. 8. PRV infection induces the accelerated loss of KIF1A protein through two separate**

784   **mechanisms.**

785   (A) In uninfected cells, KIF1A protein is inherently prone to be degraded by the proteasome. The

786   steady state concentration of KIF1A protein is achieved through rapid protein synthesis and

787   proteasomal degradation. (B) PRV infection induces KIF1A mRNA degradation and reduced

788   protein synthesis, while the existing KIF1A proteins undergo default proteasomal degradation.

789   Furthermore, the proteasomal degradation of the existing KIF1A proteins is accelerated by the

790   PRV gE/gI/US9 complex in the late phase of infection. Images were created with BioRender.

791

36

Figure 1

(A)

(B)

(C)

(D)
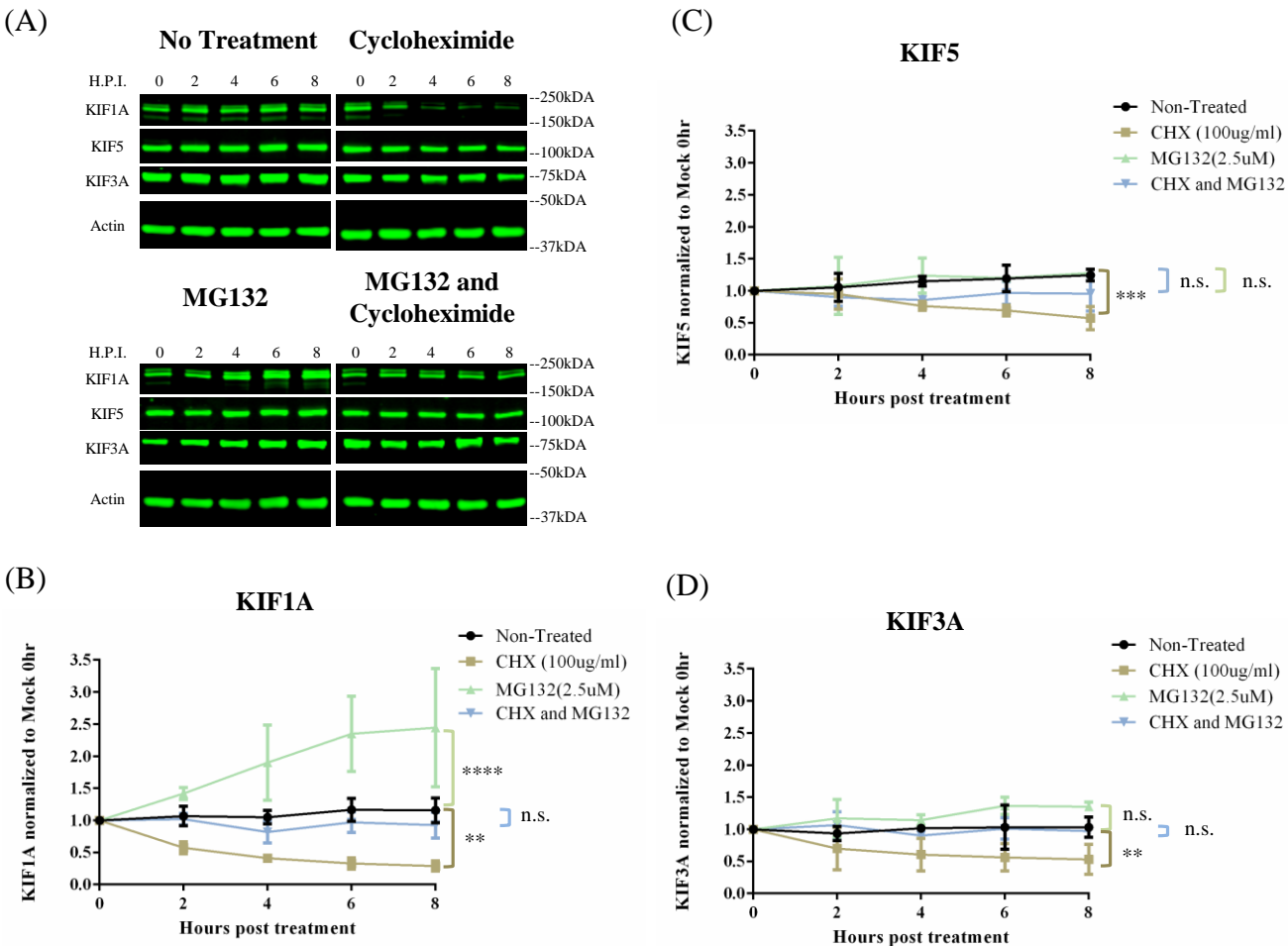
Fig. 1. KIF1A protein undergoes rapid accumulation and degradation in neuronal cells upon MG132 and CHX treatments.

Figure 2

(A)

Mock-infected

(B)

PRV Becker infection: MOI=20
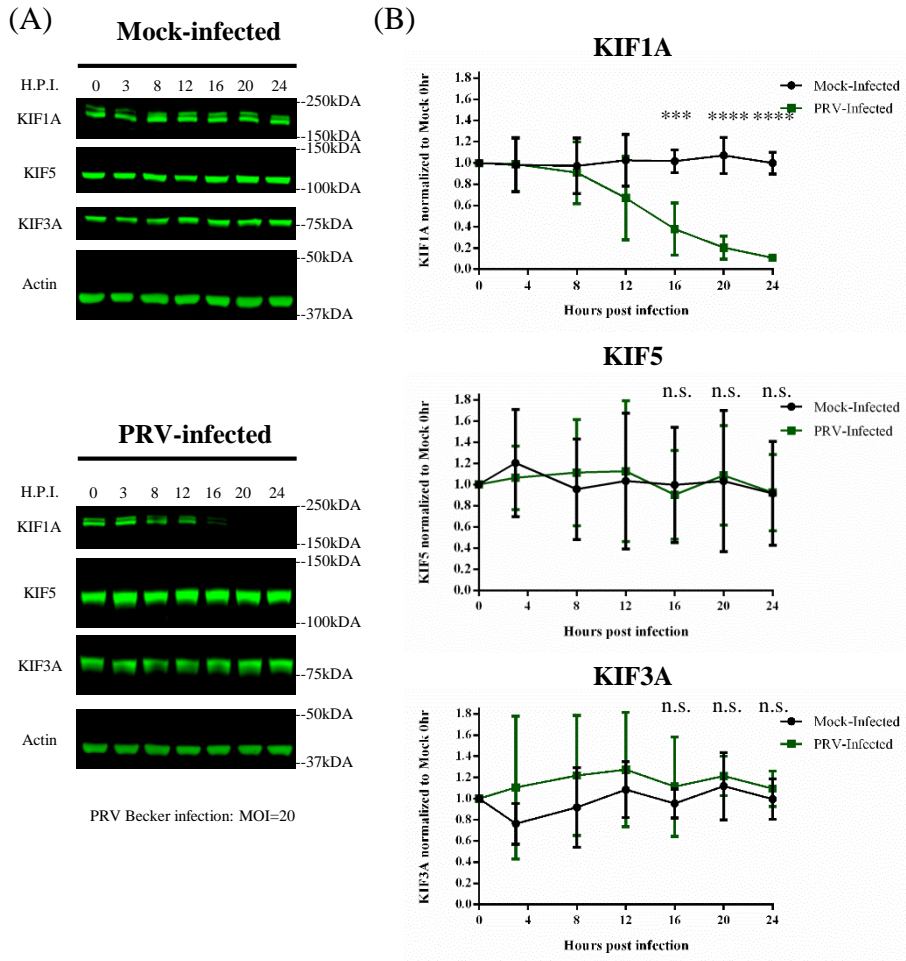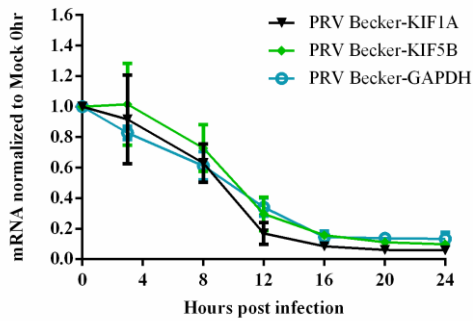
Fig. 2. KIF1A protein concentration is reduced during PRV infection in neuronal cells.

Figure 3

(A)   (B)
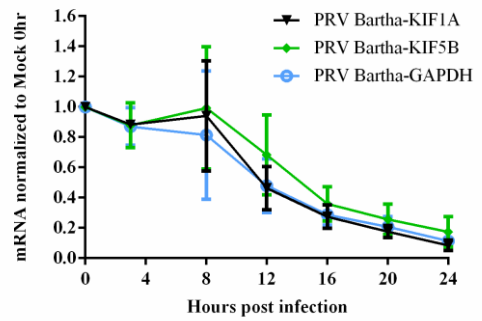
Fig. 3. The abundance of KIF1A, KIF5B, and GAPDH transcripts is significantly reduced in PRV-infected neuronal cells.

Figure 4

(A)

Mock-infected

H.P.I. 0 8 12 16 20 24

KIF1A

--250kDA
--150kDA
--250kDA

MG132 at 12 h.p.i.

--150kDA
--50kDA

Actin

--37kDA
--50kDA

MG132 at 12 h.p.i.

--37kDA

(B)

PRV-infected

H.P.I. 0 8 12 16 20 24

KIF1A

--250kDA
--150kDA
--250kDA

MG132 at 12 h.p.i.

--150kDA
--50kDA

Actin

--50kDA

MG132 at 12 h.p.i.

--37kDA

(C)
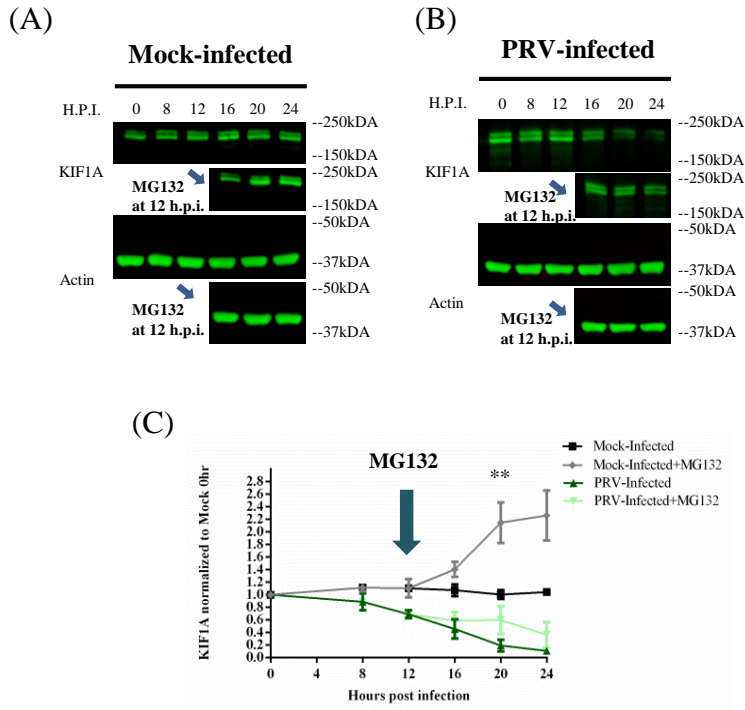
Fig. 4. KIF1A is degraded by the proteasome in the late phase of PRV infection.
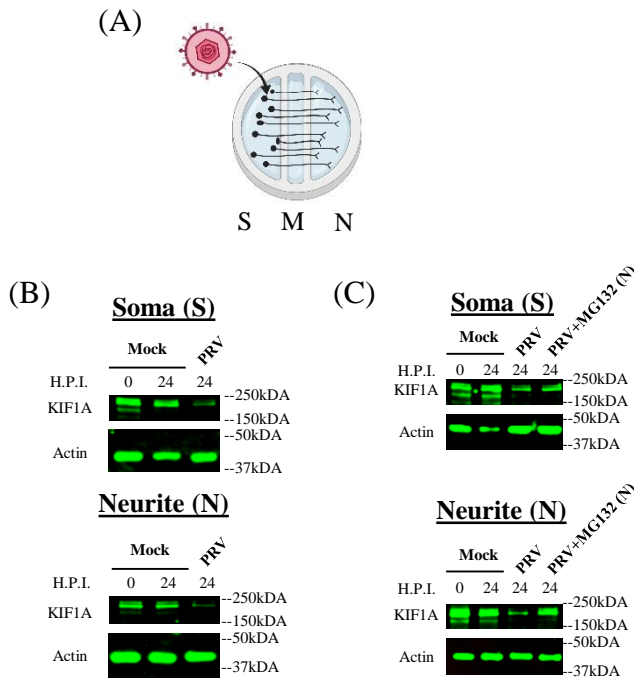
Figure 5

Fig. 5. PRV infection of compartmented primary neuronal cultures leads to reduction of KIF1A protein and proteasomal degradation in axons.

Figure 6

(A)

(B)

(C)
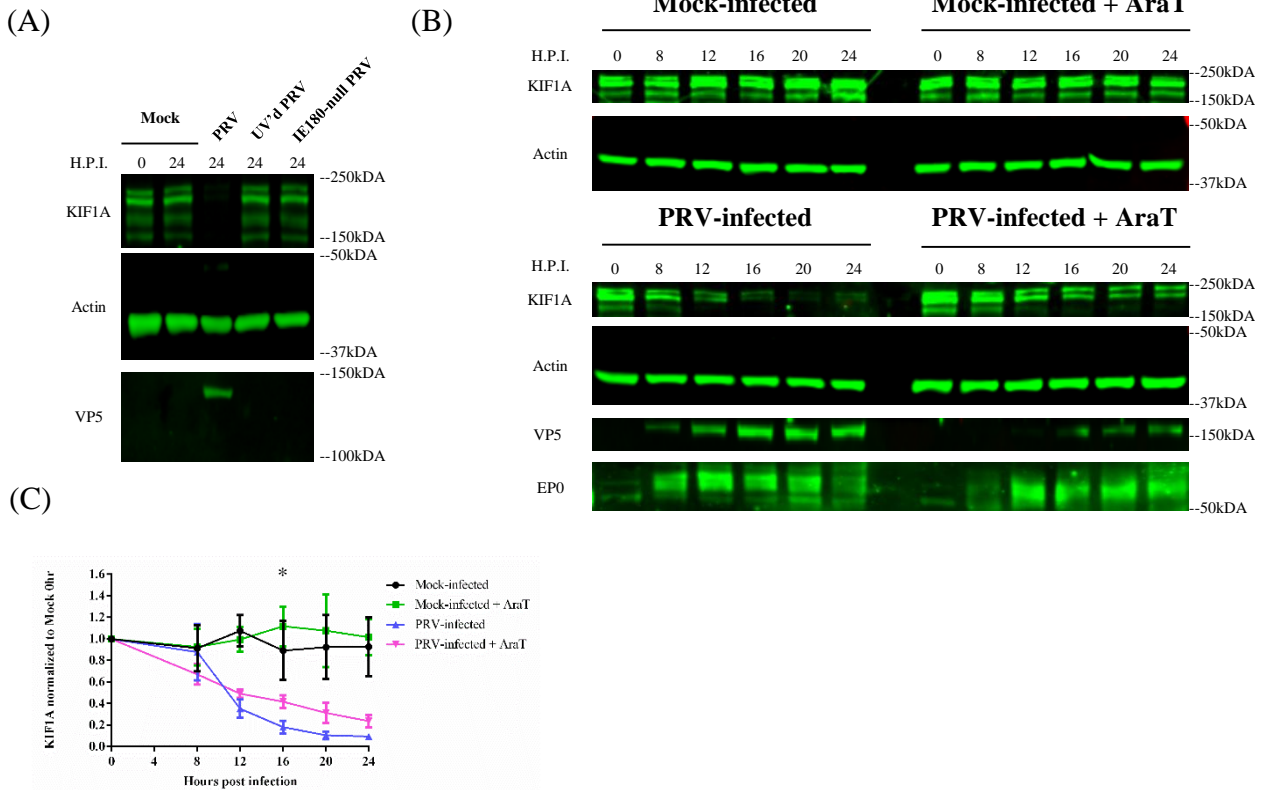
Fig. 6. Accelerated proteasomal degradation of KIF1A during infection requires the expression of both PRV early and late proteins.
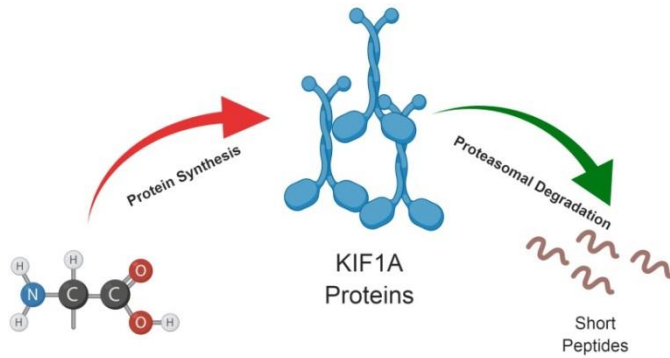
Figure 7
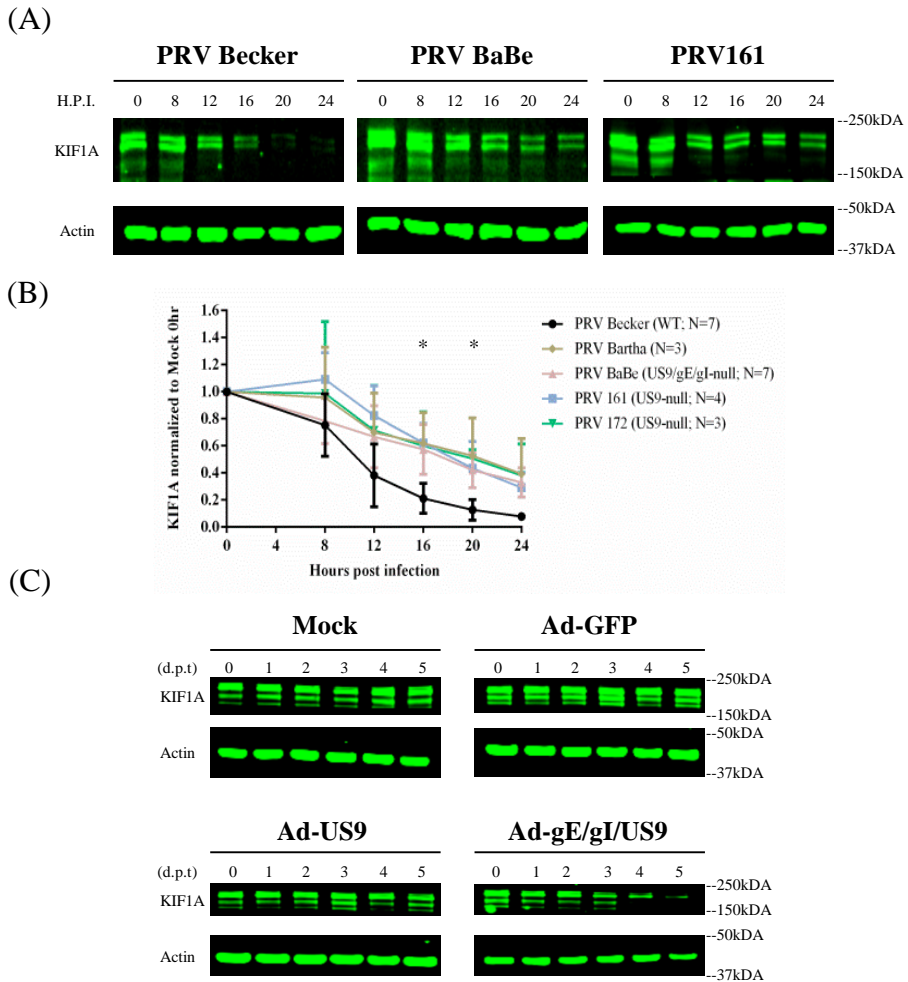
(A)

(B)

(C)

Fig. 7. PRV anterograde-spread complex US9/gE/gI promotes the accelerated degradation of KIF1A proteins.
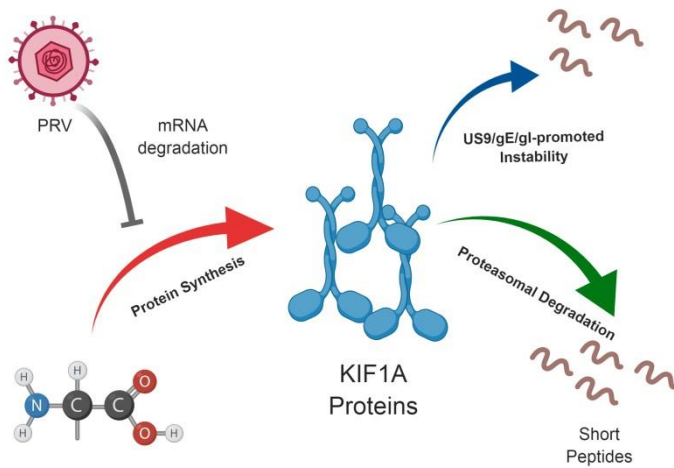
Figure 8 (MODEL)

(A)

(B)

Fig. 8. PRV infection induces the accelerated loss of KIF1A protein through two separate mechanisms.
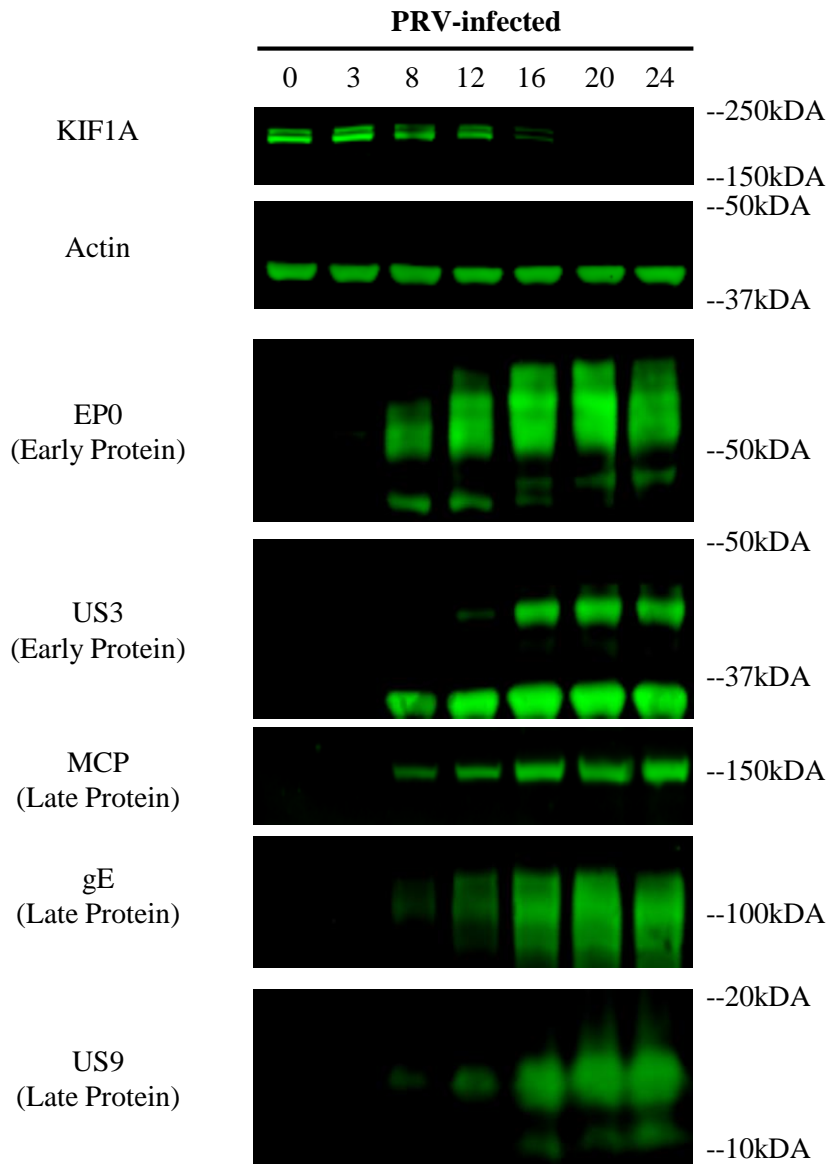
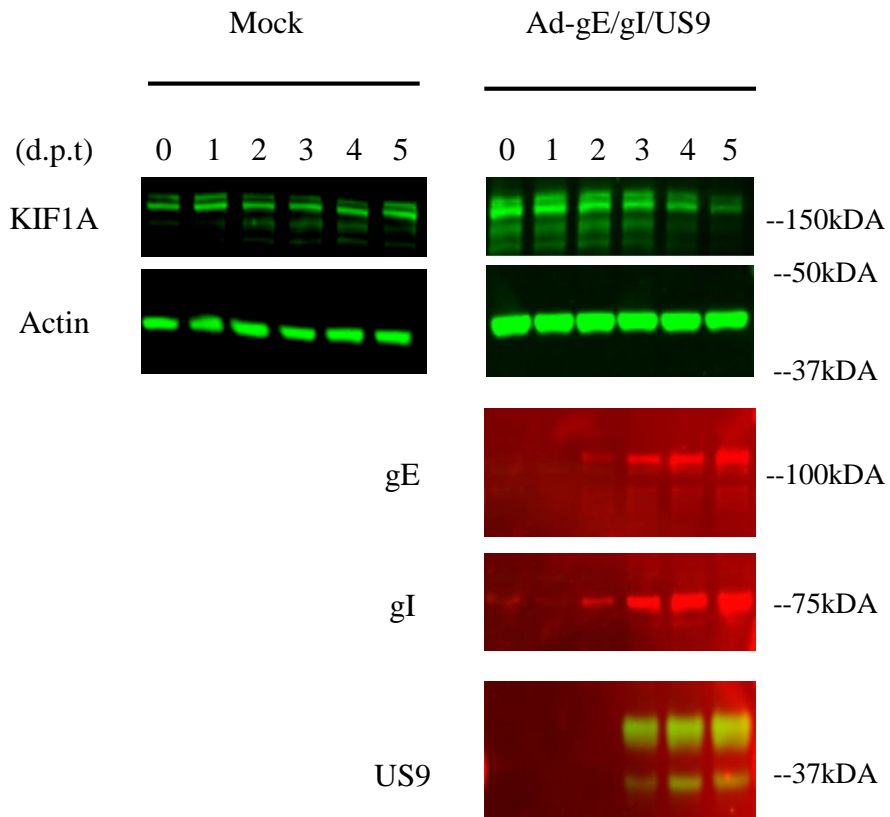Figure S1. PRV early and late gene expressions in differentiated PC12 cells.

Figure S2. Expression of transduced genes US9, gE, and gI in differentiated PC12 cells.